1-1-1989

Viscous Cross-waves: An Analytical Treatment

Andrew J. Bernoff
Harvey Mudd College

L. P. Kwok
University of Arizona

Seth Lichter
University of Arizona

Viscous cross-waves: An analytical treatment

Andrew J. Bernoff
Department of Mathematics, University of Arizona, Tucson, Arizona 85721

L. P. Kwok and Seth Lichter
Department of Aerospace and Mechanical Engineering, University of Arizona, Tucson, Arizona 85721

(Received 6 December 1988; accepted 20 December 1988)

Viscous effects on the excitation of cross-waves in a semi-infinite box of finite depth and width are considered. A formalism using matched asymptotic expansions and an improved method of computing the solvability condition is used to derive the relative contributions of the free-surface, sidewall, bottom, and wavemaker viscous boundary layers. This analysis yields an expression for the damping coefficient previously incorporated on heuristic grounds. In addition, three new contributions are found: a viscous detuning of the resonant frequency, a slow spatial variation in the coupling to the progressive wave, and a viscous correction to the wavemaker boundary condition. The wavemaker boundary condition breaks the symmetry of the linear neutral stability curve at leading order for many geometries of experimental interest.

I. INTRODUCTION

Cross-waves are a classical hydrodynamic example of parametric instability. Garrett[1] showed that cross-waves are excited within a narrow band of frequencies in a finite tank with a wavemaker at one end. Jones[2] extended these ideas to an infinite tank; he showed that a nonlinear Schrödinger (NLS) equation governed the dynamics of inviscid cross-waves. Because the boundary condition at the wavemaker introduced energy into the fluid and there was no dissipation mechanism in the inviscid theory, Jones' numerical model tended to show unbounded growth and instability. This problem can be ameliorated by the addition of viscous damping; this was done by Barnard and Pritchard[3] for the linear theory and by Barnard *et al.*[4] for the related problem of sloshing waves in an unbounded channel, which is also governed by a NLS equation. Subsequently, damping was incorporated into the NLS equation for cross-waves by Lichter and Chen[5] and Miles and Becker.[6]

All these treatments of damping were done in a qualitative fashion; it was assumed that the damping was linear, and the coefficient was evaluated empirically. A formalism for treating the viscous damping resulting from an oscillating boundary layer (Stokes layer) near a solid boundary was developed by Ursell[7] using an energy dissipation method. Similar methods exist for predicting the decay of a progressing wave.[8] Mei and Liu[9] computed the viscous damping of a surface wave confined by side walls using matched asymptotics, and showed the equivalence of this method to the energy dissipation method. They showed that the meniscus region, where the free surface meets the solid boundary, caused the same order of dissipation as the Stokes layers at the side walls. In addition, their work demonstrated that viscous effects not only damp but also detune the resonant frequency at leading order.

The purpose of the present study is to use a matched asymptotics method similar to that of Mei and Liu[9] to incorporate the leading-order viscous damping and detuning from the wavemaker, side walls, bottom, and free surface into the NLS equation for cross-waves. Jones' analysis[2] is modified to consider a finite-depth tank so bottom effects can be considered. In addition, an improved formalism for obtaining the solvability condition at each order via a Green's identity is introduced. This method, like the energy dissipation method,[10] reduces the calculation of viscous effects to a surface integral over the boundaries; the two methods are comparable in terms of length and ease of calculation.

The viscous boundary layers are matched to an irrotational core. This induces viscous corrections to the inviscid boundary conditions and, in turn, a linear viscous correction to the NLS equation. The free surface induces a damping that is inversely proportional to the Reynolds number (Re) based on cross-wave frequency and wavenumber. The damping and detuning from the solid boundaries at the side walls (including meniscus) and bottom are proportional to $1/\sqrt{\mathrm{Re}}$ and decrease inversely with width and exponentially with depth, respectively. A new contribution to the wavemaker boundary condition is found; although no dissipation occurs on the wavemaker at this order, the meniscus layer modifies the boundary layer by an order of $1/\sqrt{\mathrm{Re}}$ correction. This correction causes the neutral stability curve to be skewed, an effect that has been observed, but not explained, in many experimental studies.[11–13] In addition, it is shown that the detuning resulting from the progressing wave is now dependent on the slow spatial coordinate; this effect, although new, is presumably too small to be observed in the present experimental geometries.

This present study is limited to viscous effects. In some physical situations other dissipative mechanisms, including surface contamination and capillary hysteresis, may be as important (see the review by Miles[10]). The formalism presented here is capable of describing an essentially irrotational core matched to narrow boundary layers. Nonviscous dissipation effects could presumably be incorporated into this formalism through a more-detailed treatment of the boundary layer structure. Moreover, the present work suggests that the form of the NLS equation and corresponding wavemaker boundary condition will remain invariant, although the value of the damping constants may change. We

 0899-8213/89/040678-11$01.90

believe that a detailed comparison with experiment will have to await these modifications.

The basic formulation of the problem is presented in the next section. In Sec. III, the structure of the boundary layers at the free surface, solid boundaries, and meniscus region are derived and the corresponding correction to the inviscid boundary conditions are determined. In Sec. IV, the solution corresponding to the inhomogeneous response to the wavemaker forcing is derived,[14] including the leading-order correction resulting from viscosity. A perturbation formalism for the modulation theory is outlined and used to derive the leading-order solution; a Green's identity for the solvability condition at each order is derived. The theory is carried to third order in Sec. V, yielding the modified NLS equation and wavemaker boundary condition incorporating all the leading-order viscous effects. This theory is discussed in Sec. VI and the modified neutral stability curves are derived. Conclusions are presented in Sec. VII, and two appendices containing auxiliary calculations are presented.

II. FORMULATION

The excitation of cross-waves resulting from a planar wavemaker oscillating with frequency 2σ in a semi-infinite channel of width W and finite depth is considered. The cross-wave wavenumber is $k = N\pi/W$, where N is the mode number. The displacement of the wavemaker is given by $(a \cos 2\sigma t)$.

In order to examine the boundary layer on the wavemaker, a coordinate system that is fixed with the moving wavemaker is used. In this coordinate system, the force resulting from the wavemaker appears as a time-dependent body force. In this frame, the wavemaker can be considered as a fixed solid wall and the corresponding boundary layer can be treated using the analysis in Sec. III. Although for simplicity a planar wavemaker is considered here, the leading-order viscous dissipation is independent of wavemaker geometry; consequently, the results are immediately applicable to wavemakers whose radius of curvature is small relative to their boundary layer thickness.

The Navier–Stokes equations and boundary conditions are rendered dimensionless by the use of the characteristic length $1/k$ and time $1/\sigma$. The resulting equations are

$$\frac{\partial u_i}{\partial x_i} = 0 , \tag{1}$$

$$\frac{\partial u_i}{\partial t} + u_j \frac{\partial u_i}{\partial x_j} - 2\epsilon(e^{2it} + e^{-2it})\hat{x}_1 = -\frac{\partial p}{\partial x_i} + (\epsilon\delta)^2 \frac{\partial^2 u_i}{\partial x_j \partial x_j} . \tag{2}$$

The boundary conditions are

$$\text{at } x = 0 , \tag{3a}$$

$$u = v = w = 0 , \quad \text{at } y = 0,\ N\pi , \tag{3b}$$

$$\text{at } z = -d . \tag{3c}$$

On the free surface, $z = \eta$,

$$w = \eta_t + u\eta_x + v\eta_y , \tag{4a}$$

$$-p + (gk/\sigma^2)\eta + 2(\epsilon\delta)^2 w_z = 0 , \tag{4b}$$

$$w_x + u_z = 0 , \tag{4c}$$

$$w_y + v_z = 0 . \tag{4d}$$

Following Mei,[15] the viscous contributions to the free-surface boundary conditions have been linearized, as only their leading-order effects will be considered. Because of viscous effects, all disturbances decay far from the wavemaker,

$$u,v,w \to 0 , \quad \text{as } x \to \infty . \tag{5}$$

This replaces the radiation condition commonly used for the inviscid problem.

The problem is now specified with respect to three dimensionless parameters. The nondimensional forcing is given by

$$\epsilon = ak \ll 1 .$$

The ratio of viscous effects to forcing is given by

$$\delta = 1/\epsilon\sqrt{\mathrm{Re}} ,$$

where the Reynolds number is defined as

$$\mathrm{Re} = \sigma/\nu k^2$$

and ν is the kinematic viscosity. In addition, finite-depth effects are parametrized by d.

In the inviscid limit, the fluid is expected to approach an inviscid irrotational core with viscous effects confined to thin boundary layers. The appropriate equations in this limit are expressed in terms of the velocity potential,

$$u = \nabla\phi , \tag{6}$$

for which incompressibility requires

$$\nabla^2\phi = 0 . \tag{7}$$

The kinematic and normal stress boundary conditions can be combined and expanded[15] as

$$\begin{aligned}\phi_{tt} + \frac{gk}{\sigma^2}\phi_z = {} & 4\epsilon i(e^{2it} - e^{-2it})x + 2\epsilon(e^{2it} + e^{-2it}) \\ & \cdot(\phi_x + \phi_{xz}\eta) - \left(\phi_{tt} + \frac{gk}{\sigma^2}\phi_z\right)_z \eta \\ & - (\nabla\phi)_t^2 - \frac{1}{2}\left(\phi_{tt} + \frac{gk}{\sigma^2}\phi_z\right)_{zz}\eta^2 \\ & - (\nabla\phi)_{tz}^2\eta - \frac{1}{2}\nabla\phi\cdot\nabla(\nabla\phi)^2 , \quad \text{at } z = 0 ,\end{aligned} \tag{8}$$

where we have kept terms to third order in ϕ and η. The first two terms on the right-hand side are contributions to the potential that arise because of the nonstationary coordinate system.

At the solid walls, no flux through the boundaries requires

$$\phi_z = 0 , \quad \text{at } z = -d , \tag{9a}$$

$$\phi_y = 0 , \quad \text{at } y = 0,\ N\pi , \tag{9b}$$

and

$$\phi_x = 0 , \quad \text{at } x = 0 . \tag{9c}$$

In the next section, the leading-order viscous corrections to (8) and (9), as a result of the boundary layers on the solid walls and the free surface, are determined.

III. BOUNDARY LAYER ANALYSIS

In this section, the leading-order dissipation of an oscillatory velocity potential in the neighborhood of the solid and free-surface boundaries is computed using matched asymptotic expansions. Because the disturbance u_i is small, nonlinear interactions do not enter the expansion at leading order. Consequently, a linear analysis in the boundary layer suffices to derive the dominant dissipative contributions.

A. Free surface

Near the free surface, let $n = z/(\epsilon\delta)$ and

$$u = Ue^{i\omega t}, \quad v = Ve^{i\omega t}, \quad w = (W/\epsilon\delta)e^{i\omega t}, \quad p = Pe^{i\omega t}. \tag{10}$$

Under this scaling, the continuity equation (1) becomes

$$W_n = -(\epsilon\delta)^2(U_x + V_y). \tag{11}$$

The momentum equation (2) yields

$$i\omega U - U_{nn} = -P_x + (\epsilon\delta)^2(U_{xx} + U_{yy}), \tag{12a}$$

$$i\omega V - V_{nn} = -P_y + (\epsilon\delta)^2(V_{xx} + V_{yy}), \tag{12b}$$

$$i\omega W - W_{nn} = -P_n + (\epsilon\delta)^2(W_{xx} + W_{yy}). \tag{12c}$$

For the free surface, it is sufficient to consider the dissipation of a two-dimensional disturbance. It is therefore assumed that $V \equiv 0$ and no variation occurs in the y direction.

In the interior of fluid, $\nabla^2\phi = 0$, and near $z = 0$, ϕ can be expanded:

$$\phi = [A(x) + B(x)z - A_{xx}(z^2/2) - B_{xx}(z^3/6) + \cdots]e^{i\omega t}, \tag{13}$$

where $A(x) = \phi(x,0)$ and $B(x) = \phi_z(x,0)$.

In the boundary layer, U, W, and P are now expanded in powers of $(\epsilon\delta)^2$:

$$(U,W,P) = (U_0,W_0,P_0) + (\epsilon\delta)^2(U_1,W_1,P_1) + \cdots. \tag{14}$$

Substituting (14) into (11) and (12), retaining the leading-order terms, and solving, yields

$$P_0 = a(x) + b(x)n, \tag{15a}$$

$$W_0 = -b(x)/i\omega, \tag{15b}$$

$$U_0 = -a_x/i\omega - b_x n/i\omega + c(x)e^{\alpha n}, \tag{15c}$$

where a, b, and c are functions of x to be determined through matching and $\alpha = \sqrt{i\omega} = (1+i)(\omega/2)^{1/2}$. Collecting terms of order $(\epsilon\delta)^2$ from (11) and (12) yields an inhomogeneous problem for (U_1,W_1,P_1); this can be solved to yield

$$P_1 = -a_{xx}(n^2/2) - b_{xx}(n^3/6), \tag{16a}$$

$$W_1 = \frac{a_{xx}n}{i\omega} + \frac{b_{xx}}{i\omega}\frac{n^2}{2} - \frac{c_x}{\alpha}e^{\alpha n}, \tag{16b}$$

$$U_1 = \frac{a_{xxx}n^2}{2i\omega} + \frac{b_{xxx}n^3}{6i\omega} - \frac{c_{xx}n}{2\alpha}e^{\alpha n}. \tag{16c}$$

Now consider (u,w) in the matching region where $1 \gg -z \gg \epsilon\delta$. Equations (15) and (16) yield

$$u = \left\{\frac{1}{i\omega}\left[\left(a_x - a_{xxx}\frac{z^2}{2}\right)\epsilon\delta + \left(b_x z + \frac{b_{xxx}z^3}{6}\right)\right] + O(z^4, e^{z/\epsilon\delta})\right\}e^{i\omega t} \tag{17a}$$

and

$$w = \left\{-\frac{1}{i\omega}\left[-\epsilon\delta a_{xx}z + \left(b - \frac{b_{xx}z^2}{2}\right)\right] + O(z^3, e^{z/\epsilon\delta})\right\}e^{i\omega t}. \tag{17b}$$

Remembering that $u = \nabla\phi$ and matching to (10) yields the identification

$$a = -i\omega\phi(x,0) \tag{18a}$$

and

$$b = -(\epsilon\delta)i\omega\phi_z(x,0). \tag{18b}$$

The free-surface boundary conditions are now applied to determine the relationship between a, b, and c. The boundary conditions are linearized and applied at $n = 0$ to reveal the leading-order viscous contributions. The tangential stress condition (4c) yields

$$U_n + W_x = 0, \tag{19}$$

which implies from (15) that

$$c = 2b_x\alpha/i\omega + O[(\epsilon\delta)^2]. \tag{20}$$

The normal stress condition (4b) and the kinematic condition (4a) can now be linearized, rescaled, and combined to yield

$$(\epsilon\delta)^{-1}(gk/\sigma^2)W - i\omega P = -2W_n. \tag{21}$$

Substituting (15) and (16) into (19) and applying conditions (18) and (20) yields

$$(gk/\sigma^2)\phi_z(x,0) - \omega^2\phi(x,0) = 4(\epsilon\delta)^2 i\omega\phi_{xx}(x,0) + O[(\epsilon\delta)^3], \quad \text{at } z = 0, \tag{22}$$

where the right-hand side of (22) is the leading-order viscous correction to the inviscid free-surface boundary condition.

B. Solid boundary

We now consider the boundary layer above a solid boundary at $z = 0$. The disturbance is assumed to be oscillatory with frequency ω. The velocity potential is expanded near $z = 0$ as

$$\phi = [\phi(x,y,0) + \phi_z(x,y,0)z + \cdots]e^{i\omega t}. \tag{23}$$

The velocity is again scaled as in (10). The problem is now specified by the continuity and momentum equations (11) and (12), together with boundary conditions $U = V = W = 0$ at $n = 0$. The leading-order solution is found:

$$P = A(x,y) + O[(\epsilon\delta)^2], \tag{24a}$$

$$U = [(i/\omega)A_x](1 - e^{-\alpha n}) + O[(\epsilon\delta)^2], \tag{24b}$$

$$V = [(i/\omega)A_y](1 - e^{-\alpha n}) + O[(\epsilon\delta)^2], \tag{24c}$$

$$W = [i(\epsilon\delta)^2/\omega](A_{xx} + A_{yy})[(1/\alpha)(1 - e^{-\alpha n}) - n] + O[(\epsilon\delta)^4]. \tag{24d}$$

Matching (24a)–(24c) with Eq. (23) yields $A = -i\omega\phi(x,y,0)$. Matching (24d) with (23) and recognizing that $\phi_{zz} = -(\phi_{xx} + \phi_{yy})$ yields

$$\alpha\phi_z(x,y,0) + (\epsilon\delta)\phi_{zz}(x,y,0) = O[(\epsilon\delta)^2, e^{-z/\epsilon\delta}] \quad (25)$$

as the boundary condition for the solid boundary.

This analysis can also be applied to the boundary layer at the side walls and wavemaker if $\partial/\partial z$ is interpreted as the derivative normal to the boundary. Equations (22) and (25) can now be used to incorporate the leading-order viscous effects into the inviscid problem, as specified by (7)–(9).

C. Meniscus region

Following Mei and Liu,[9] the contribution to viscous damping from the meniscus region, where the free surface joins a vertical solid boundary, is now computed. In Sec. III B, it was seen that within a distance $O(\epsilon\delta)$ of the solid boundary, there is an additional contribution to the velocity field as a result of the vorticity generated at the boundary. Although the velocity in this region is $O(1)$, it is confined to a thin layer and contributes only a small correction to the free-surface condition, which is now computed. Without loss of generality, the region near where the free surface ($z=0$) intersects the side wall ($y=0$) is considered. The analysis on the opposing side wall and at the wavemaker is similar.

From Eq. (24), the additional contribution to the velocity normal to the surface near the wall can be computed,

$$w = w_M + \phi_z\,, \quad (26)$$

where w_M, the contribution from the meniscus, is given by

$$w_M = -\phi_z e^{-\zeta} \quad (27)$$

and ζ is the scaled coordinate normal to the solid boundary,

$$\zeta = \alpha y/\epsilon\delta\,. \quad (28)$$

If w_M is now incorporated into the analysis of Sec. III A, an additional contribution to the free-surface boundary condition (22) is generated by the W term in Eq. (21),

$$(gk/\sigma^2)\phi_z(x,0) - \omega^2\phi(x,0) = -(gk/\sigma^2)w_M(x,0)\,, \quad \text{at } z=0\,. \quad (29)$$

Although $w_M = O(1)$ in the boundary layer, it will contribute an $O(\epsilon\delta)$ viscous correction to the analysis because it is confined to the thin region [thickness $= O(\epsilon\delta)$].

Equations (22), (25), and (29) now specify how leading-order viscous effects from the free surface, solid boundaries, and meniscus regions, respectively, modify the boundary conditions for the inviscid problem.

IV. DERIVATION OF THE VISCOUS MODULATION THEORY

In this section, the viscous boundary layer terms computed above are incorporated into the modulation theory.

A. Scaling

Following the work of Jones,[2] variables ϕ, η, and σ are now expanded in powers of ϵ such that

$$\begin{aligned}\phi &= \epsilon\phi_1 + \epsilon^2\phi_2 + \epsilon^3\phi_3 + \cdots\,,\\ \eta &= \epsilon\eta_1 + \epsilon^2\eta_2 + \cdots\,,\\ \sigma &= \sigma_0(1 + \epsilon^2\sigma_2 + \cdots)\,,\end{aligned} \quad (30)$$

where $\sigma_0 = [gk\tanh(d)]^{1/2}$ is the cutoff frequency. At the same time, multiple scales

$$\chi = \epsilon x\,, \quad \tau = \epsilon t\,, \quad \text{and} \quad \tau' = \epsilon^2 t \quad (31)$$

are also introduced.

Equation (7) now reads

$$\nabla^2\phi = \frac{\partial^2\phi}{\partial x^2} + 2\epsilon\frac{\partial^2\phi}{\partial x\,\partial\chi} + \epsilon^2\frac{\partial^2\phi}{\partial\chi^2} + \frac{\partial^2\phi}{\partial y^2} + \frac{\partial^2\phi}{\partial z^2} = \Delta\phi + 2\epsilon\frac{\partial^2\phi}{\partial x\,\partial\chi} + \epsilon^2\frac{\partial^2\phi}{\partial\chi^2}\,, \quad (32)$$

where $\Delta\phi$ is the Laplacian in the (x,y,z) coordinates.

We now proceed to solve Eq. (32) in successive powers of ϵ. Note that ϕ is real, but it is convenient to separate the solution by frequency dependencies, $e^{i\omega t}$. Consequently, at each order, ϕ will be expressed as a sum of frequency components together with their complex conjugates (denoted as c.c.).

B. First-order solution

The leading-order solution consists of an inhomogeneous response at the wavemaker frequency[14] ($\phi_i e^{2it}$ + c.c.), together with a homogeneous cross-wave solution ($\phi_h e^{it}$ + c.c.).[1] As the problem is now being considered in a moving frame, an additional contribution to the velocity potential ($-ixe^{2it}$ + c.c.) is induced,

$$\phi_1 = -ixe^{2it} + \phi_i e^{2it} + \phi_h e^{it} + \text{c.c.} \quad (33)$$

The equations specifying ϕ_i are

$$\Delta\phi_i = 0\,, \quad (34)$$

with the free-surface boundary condition

$$-4\phi_i + H\phi_{i_z} = (\epsilon\delta)^2 8i\phi_{i_{xx}} + \sum_j H\phi_z e^{-\zeta_j}\,, \quad \text{at } z=0\,, \quad (35a)$$

where $H = gk/\sigma_0^2 = 1/\tanh(d)$, and the sum is taken over the meniscus layer for the two side walls with ζ_j being the scaled outward normal (cf. Sec. III C). The remaining boundary conditions are

$$\phi_{i_x} = i\,, \quad \text{at } x=0\,, \quad (35b)$$

$$\phi_{i_z} = \epsilon\delta[(1-i)/2]\phi_{i_{zz}}\,, \quad \text{at } z=-d\,, \quad (35c)$$

$$\phi_{i_y} = 0\,, \quad \text{at } y=0, N\pi\,, \quad (35d)$$

together with

$$\phi_i \to 0\,, \quad \text{as } x\to\infty\,. \quad (35e)$$

In Eqs. (35a)–(35c), respectively, the viscous corrections that follow from (22), (25), and (29) have been included. Although these corrections enter formally at a higher order, including them here avoids the introduction of a singular perturbation.

A uniform leading-order solution for ϕ_i is given by

$$\phi_i = Be^{\gamma x}\frac{\cosh[m(z+d)]}{\cosh(md)}e^{-imx} + \sum_j iB_j e^{-m_j x}\frac{\cos[m_j(z+d)]}{\cos(m_j d)} + O(\epsilon)\,, \quad (36)$$

where γ is given by

$$\gamma = \frac{-2m^3\epsilon\delta^2 - (1+i)\delta/(N\pi \tanh md) - (1+i)\delta m^2/\sinh 2md}{1 + 2md/\sinh 2md}. \tag{37}$$

The solution for ϕ_i (36) consists of a damped progressing wave and a sum of parasitic modes localized on the wavemaker. Because the dissipation on the free surface and bottom was included at this order, the solution (36) modifies that of Havelock to include the slow decay ($e^{\gamma\chi}$) of the progressing wave. The B and B_j's are determined from eigenfunction expansions and are given in Appendix A, together with eigenvalues m and m_j's.

The forcing frequency σ_0 has been chosen so that the leading-order cross-wave equations admit a homogeneous cross-wave solution, $\phi_h e^{it}$ + c.c., which satisfies

$$\Delta\phi_h = I_1 \tag{38}$$

$$-\phi_h + H\phi_{h_z} = I_2, \quad \text{at } z = 0, \tag{39a}$$

$$\phi_{h_z} = I_3, \quad \text{at } z = -d, \tag{39b}$$

$$\phi_{h_x} = I_4, \quad \text{at } x = 0, \tag{39c}$$

$$\phi_{h_y} = I_5, \quad \text{at } y = 0, \tag{39d}$$

$$\phi_{h_y} = I_6, \quad \text{at } y = N\pi, \tag{39e}$$

together with

$$\phi_h \to 0, \quad \text{as } x \to \infty, \tag{39f}$$

and with $I_j = 0$. This admits a solution

$$\phi_h = A(\chi,\tau,\tau')\,\hat{\phi}(z,y), \tag{40}$$

where

$$\hat{\phi} = [\cosh(z+d)/\cosh d\,]\cos y \tag{41}$$

and A is a complex modulation amplitude, which is allowed to vary on the slow time and space scales. Note that to satisfy (39), it will be assumed that

$$A \to 0 \quad \text{as } \chi \to \infty. \tag{42}$$

At the nth order of perturbation theory, it is necessary to solve for ϕ_n by inverting the same linear problem that specified ϕ_1. The solution for ϕ_n is specified by inhomogeneous functions of ϕ_1 through ϕ_{n-1}. Because the e^{it} portion of this problem has a homogeneous solution, a solvability condition is needed to allow the inversion of the linear operator. This solvability condition is now derived.

Consider the linear problem (38) and (39) with ϕ_h replaced by an unknown function ψ and I_1 through I_6 representing inhomogeneities in the equation and boundary conditions. The problem is self-adjoint and, as such, the Fredholm alternative implies that the solvability condition on the $\hat{\phi}$ subspace is given by considering

$$\int_0^L dx \int_0^{N\pi} dy \int_{-d}^0 dz\, \Delta\hat{\phi}\,\psi = 0, \tag{43}$$

where L is taken sufficiently large to be in the far field (far from the wavemaker) where all the disturbances are exponentially small. By applying the Green's theorem to (43) and using (39), the unknown ψ can be eliminated to yield

$$\int_0^L dx \int_0^{N\pi} dy \int_{-d}^0 dz\, \hat{\phi} I_1 - \int_0^{N\pi} dy \int_0^L dx \frac{\hat{\phi} I_2}{H}\bigg|_{z=0} + \int_0^{N\pi} dy \int_0^L dx\, \hat{\phi} I_3\bigg|_{z=-d} + \int_0^{N\pi} dy \int_{-d}^0 dz\, \hat{\phi} I_4\bigg|_{x=0} + \int_{-d}^0 dz \int_0^L dx\, \hat{\phi} I_5\bigg|_{y=0} - \int_{-d}^0 dz \int_0^L dx\, \hat{\phi} I_6\bigg|_{y=N\pi} = 0. \tag{44}$$

This solvability condition can now be applied directly to the e^{it} component solution at each order.

C. Second-order solution

At second order, a number of inhomogeneities appear in the boundary conditions that lead to a nontrivial solvability condition. In the interior of the fluid,

$$\Delta\phi_2 = 0. \tag{45}$$

On the free surface, the quadratic interactions of ϕ_1 in (8) must be retained. In addition, there is a contribution from the potential term, the τ time scale, and from the meniscus region of the side walls and wavemaker (cf. Sec. III C)

$$\phi_{2_{tt}} + H\phi_{2_z} = -\eta_1(\phi_{1_{tz}} + H\phi_{1_{zz}}) - 2(\phi_{1_x}\phi_{1_{xt}} + \phi_{1_y}\phi_{1_{yt}} + \phi_{1_z}\phi_{1_{zt}}) + 2(e^{2it} + e^{-2it})\phi_{1_x} - 2\phi_{1_{tt}} + \sum_j H\frac{\phi_z}{\epsilon}e^{-\zeta_j}, \quad \text{at } z = 0. \tag{46}$$

The sum in the last term is taken over the three meniscus regions along the wavemaker and along the two side walls, and ζ_j is the scaled coordinate perpendicular to the solid boundary for each of these regions (cf. Sec. III C).

The viscous contributions on the solid boundaries can be computed using (25). On the bottom,

$$\phi_{2_z} = -\delta[(1-i)/\sqrt{2}]\phi_{h_{zz}}e^{it} + \text{c.c.}, \quad \text{at } z = -d. \tag{47}$$

Similarly, on the side walls,

$$\phi_{2_y} = -\delta[(1-i)/\sqrt{2}]\phi_{h_{yy}}e^{it} + \text{c.c.}, \quad \text{at } y = 0, \tag{48a}$$

$$\phi_{2_y} = \delta[(1-i)/\sqrt{2}]\phi_{h_{yy}}e^{it} + \text{c.c.}, \quad \text{at } y = N\pi. \tag{48b}$$

On the wavemaker, note that $\phi_{h_{xx}} = O(\epsilon^2)$ because the cross-wave solution is only a function of the slow length scale χ. Consequently,

$$\phi_{2_x} = -\phi_{1_y}, \quad \text{at } x = 0. \tag{49}$$

To obtain the solvability condition at order ϵ^2, the e^{it} component of (45)–(49) must be considered; this component of ϕ_2 will be labeled ϕ_{21}, i.e.,

$$\phi_2 = \phi_{21}e^{it} + \text{c.c.} + \text{nonresonant terms}. \tag{50}$$

From (45),

$$\Delta\phi_{21} = 0 . \tag{51}$$

From (46), the only terms that have the correct time dependence are quadratic interactions of terms in ϕ_h proportional to $A^* e^{-it}$, with terms in ϕ_i proportional to e^{2it}, the τ derivative of ϕ_h, and meniscus contributions,

$$\begin{aligned} -\phi_{21} + H\phi_{21_z} &= iA^* \cos y\left[(2+6H^{-2})\phi_i - \phi_{i_{zz}}\right] - 2iA_\tau \cos y \\ &\quad + (A/\epsilon)(e^{-\kappa y} + (-1)^N e^{\kappa(y-N\pi)} + e^{-\kappa x}\cos y) , \end{aligned} \tag{52}$$

where κ is given by

$$\kappa = (1+i)/\sqrt{2}](\epsilon\delta)^{-1} . \tag{53}$$

From (47)–(49) the e^{it} component yields

$$\phi_{21_z} = -\delta[(1-i)/\sqrt{2}]A(\cos y/\cosh d), \quad \text{at } z = -d , \tag{54}$$

$$\phi_{21_y} = \delta[(1-i)/\sqrt{2}]A\,[\cosh(z+d)/\cosh d\,] , \quad \text{at } y = 0 , \tag{55a}$$

$$\phi_{21_y} = -[\delta(1-i)/\sqrt{2}]A\,[\cosh(z+d)/\cosh d\,](-1)^N , \quad \text{at } y = N\pi , \tag{55b}$$

$$\phi_{21_x} = -A_\chi[\cosh(z+d)/\cosh d\,]\cos y , \quad \text{at } x = \chi = 0 . \tag{56}$$

Applying condition (44) and using (52)–(56) to evaluate I_j, yields the solvability condition at second order,

$$-\frac{SN\pi}{4H}(A_\chi + RA^* + D_1A)\Big|_{x=\chi=0} + \int_0^L dx\,\frac{N\pi i}{H}\{A_\tau + D_2A\} = 0 , \tag{57}$$

where

$$\begin{aligned} R &= \frac{2i}{S}\int_0^L dx\left[\phi_{i_{zz}} - (2+6H^{-2})\phi_i\right] \\ &= \frac{1}{S}[d(H+3H^{-1}) - 2] , \end{aligned} \tag{58}$$

$$D_1 = [\delta(1-i)/\sqrt{2}](2/S) , \tag{59}$$

$$D_2 = \frac{\delta(1+i)}{\sqrt{2}}\left[\frac{1}{\sinh(2d)} + \frac{1}{N\pi}\left(1 - \frac{2d}{\sinh 2d}\right)\right] , \tag{60}$$

and

$$S = 1 + 2d/\sinh 2d . \tag{61}$$

The terms (57) can be traced to the various inhomogeneities; the A_χ term is a result of the wavemaker inhomogeneity (56), the RA^* term is generated by the ϕ_i,ϕ_h^* interaction in the free-surface boundary condition, and the D_1 term is generated by the meniscus region on the wavemaker through the free-surface condition. Inside the integral, the A_τ term is generated by the slow τ derivative in the free-surface condition, while D_2 contains contributions from the side wall meniscus region, the side wall conditions (55a) and (55b), and the bottom boundary condition (54). The expression for R (58) is evaluated using the identities developed in Appendix A.

Equation (57) can be satisfied by setting both the constant term at $x = \chi = 0$,

$$A_\chi = -RA^* - D_1A , \tag{62}$$

and the integrand of the x integral,

$$A_\tau + D_2A = 0 , \tag{63}$$

to zero. Equation (63) is now the leading-order evolution equation for A, and Eq. (62) is its boundary condition at $\chi = 0$.

Note that the magnitude of the contribution from the meniscus on the wavemaker D_1 only varies between δ and $\delta/2$ as the depth changes from shallow to deep. However, the dissipation resulting from the side walls and bottom D_2 is a strong function of the geometry. The first term in (60) is the dissipation from the bottom; as can be anticipated,[9] its effect decreases exponentially with increasing depth as a result of the exponential decrease in the potential. The second term represents the dissipation resulting from the side walls, including the meniscus region; it decreases inversely with the mode number N or equivalently inversely with the width of the tank at a fixed wavelength.

Note that the real part of D_2 is positive and, consequently, all solutions to (63) will decay. However, if $|D_2| \lesssim \epsilon$, the next-order correction to (63) may overcome the damping as a result of D_2. This will be the case whenever the tank is sufficiently wide and deep, or if $\delta \lesssim \epsilon$, corresponding to $(\mathrm{Re})^{-1/2} \lesssim \epsilon^2$. To compute the next-order correction to Eq. (63), the second-order solution ϕ_2 must be determined and a solvability condition for $O(\epsilon^3)$ must be derived.

Because the solvability condition (57) is satisfied, the second-order solution ϕ_2 could now be computed in its entirety. However, as is clear from Jones,[2] many portions of ϕ_2 will not contribute to resonances at order ϵ^2. Moreover, many of the components of ϕ_2 are localized on the wavemaker and yield only small corrections to the boundary condition (62) and, consequently, are not of importance. Additionally, there are higher-order corrections to the viscous dissipation from the side walls and bottom; these can be neglected relative to D_2. The remaining terms in ϕ_2 are all generated by cross-wave–cross-wave, cross-wave–progressing wave, or progressing wave–progressing wave interactions. These are computed in Appendix B.

V. THIRD-ORDER SOLUTION

In this section a portion of the solvability condition for the third-order problem is computed. In particular, the nonlinear interaction of cross-waves and progressing waves, the slow variation in χ, the effect of frequency detuning, and the leading-order contribution of viscous damping as a result of the free surface are computed. A number of terms that are always formally small relative to the second-order dissipation term will not be presented here; they have been computed elsewhere.[16] Specifically, the contribution to (63), as a result of the higher-order interactions of the viscous boundary layers on the solid walls, are of the form

$$(\text{third-order contribution}) \sim \epsilon(D_2)^2A \ll D_2A .$$

In addition, the term $\phi_{1_{\tau\tau}}$ is omitted from the free-surface

boundary condition because it yields a negligible contribution of the form

$$\epsilon A_{\tau\tau} \approx -\epsilon D_2 A_\tau \approx \epsilon (D_2)^2 A \ll D_2 A ,$$

where (63) has been used to eliminate the time derivatives.

In the interior of the fluid, the slow variation in χ enters as an inhomogeneity,

$$\Delta\phi_3 = -\phi_{1_{YY}} . \tag{64}$$

The appropriate boundary conditions are

$$\phi_{3_y} = 0 , \quad \text{at } y = 0, N\pi , \tag{65}$$

$$\phi_{3_z} = 0 , \quad \text{at } z = -d , \tag{66}$$

$$\begin{aligned} &\phi_{3_{tt}} + H\phi_{3_z} \\ &\quad = -2\phi_{1_{t\tau}} + 2H\sigma_2\phi_{1_z} - (\phi_{1_{tt}} + H\phi_{1_z})_z \eta_2 \\ &\qquad - (\phi_{2_{tt}} + H\phi_{2_z})_z \eta_1 - 2(\nabla\phi_1 \cdot \nabla\phi_2)_t - (\nabla\phi_1)^2_{tz}\eta_1 \\ &\qquad - \tfrac{1}{2}\nabla\phi_1 \cdot \nabla(\nabla\phi_1)^2 - 4\delta^2\phi_{1_{zzt}} , \quad \text{at } z = 0 . \end{aligned} \tag{67}$$

In (67), the slow time scale (τ'), the frequency detuning (ϕ_2), possibly resonant nonlinear interactions of ϕ_1 and ϕ_2, and the viscous free-surface contributions, have been retained.

Substituting for ϕ_1 and ϕ_2 and retaining resonant (e^{it}) terms yields

$$\Delta\phi_3 = -A_{\chi\chi} e^{it} [\cosh(z+d)/\cosh d] \cos y , \tag{68}$$

with the free-surface boundary condition

$$\begin{aligned} \phi_{3_{tt}} + H\phi_{3_z} = \{ &-2iA_\tau + 2\sigma_2 A + J_a e^{2\gamma_R \chi} A \\ &+ J_b A |A|^2 - 4i\delta^2 A \} \cos y \, e^{it} , \end{aligned} \tag{69}$$

where

$$\begin{aligned} J_a = B^2 \{ &[2(m^2 - 24/H^2) + (1 - 9/H^2)(M-5)] \\ &\cdot [8 + (M-5)m^2 + 24(2-M)/H^2] \\ &\cdot [(M-5)^2 - 16]^{-1} + 32/H^4 \} \end{aligned} \tag{70}$$

and

$$J_b = (6H^{-4} - 5H^{-2} + 16 - 9H^2)/8 , \tag{71}$$

with $M = sH \tanh(sd)$, $s = (m^2+1)^{1/2}$, and $\gamma_R = \mathrm{Re}\{\gamma\}$. Applying (44) yields the solvability condition

$$\begin{aligned} \frac{N\pi}{2H} \int_0^L dx \Big(&-\frac{S}{2} A_{\chi\chi} + 2iA_\tau - 2\sigma_2 A \\ &- J_a e^{2\gamma_R \chi} A - J_b A |A|^2 + 4i\delta^2 A \Big) = 0 . \end{aligned} \tag{72}$$

Solvability condition (72) can only be satisfied if the integrand is identically zero, i.e., if

$$\begin{aligned} 2iA_\tau = (S/2)A_{\chi\chi} + (2\sigma_2 + J_a e^{2\gamma_R \chi} - 4i\delta^2)A \\ + J_b A |A|^2 . \end{aligned} \tag{73}$$

It is desirable to combine (63) and (73) into a single amplitude equation for A; this can be done by replacing $A(\chi,\tau,\tau')$ by $A(\chi,T)$, where $T = \epsilon^2 t$ is a single long time scale. This yields the relation

$$\partial_T = (1/\epsilon)\partial_\tau + \partial_{\tau'} . \tag{74}$$

Using (74) to combine (63) and (73) now yields

$$iA_T = \frac{S}{4} A_{\chi\chi} + \left(\sigma_2 + \frac{J_a}{2} e^{2\gamma_R \chi} - iD_0 \right) A + \frac{J_b}{2} A |A|^2 , \tag{75}$$

where

$$\begin{aligned} D_0 &= \frac{D_2}{\epsilon} + 2\delta^2 \\ &= \frac{\delta}{\epsilon} \frac{1+i}{\sqrt{2}} \left[\frac{1}{\sinh(2d)} + \frac{1}{N\pi} \left(1 - \frac{2d}{\sinh 2d} \right) \right] + 2\delta^2 , \end{aligned} \tag{76}$$

with boundary conditions

$$A_\chi = -RA^* - D_1 A , \quad \text{at } \chi = 0 \tag{77a}$$

and

$$A \to 0 , \quad \text{as } \chi \to \infty . \tag{77b}$$

VI. DISCUSSION AND LINEAR ANALYSIS

A. Comparison to previous work

Equations (75)–(77) describe the evolution of viscous cross-waves in a finite-depth box. Far from the wavemaker, both the progressing wave and parasitic modes become exponentially small, leaving a standing wave in a channel modulated in the transverse direction. In the inviscid limit, this problem was considered by Larraza and Putterman,[17] and their Eq. (15) is identical, after rescaling, to (75), with viscous effects suppressed. Larazza and Putterman[17] noted that the coefficient of the nonlinear term J_b is negative for $0 < d < 1.022$ (our notation) and positive for greater d; the same is true here, and a similar qualitative change in the dynamics may be expected.

Earlier work on cross-waves has concentrated on the infinite-depth case with an arbitrarily shaped wavemaker[2,5,6] In the limit of large depth, the geometry considered here can be related to the case of a planar wavemaker of depth d in an infinitely deep tank. Because the velocity potential decreases rapidly with depth, the difference between the coefficients S, J_a, J_b, and R in these two cases is exponentially small in this limit.

The real part of D_0 takes the form of the heuristic damping postulated by previous authors.[5,6] Three new effects are seen here: a viscous detuning corresponding to the imaginary part of D_0, a viscous correction to the wavemaker boundary conditions as given by D_1 in (77a), and a slow spatial decay of the progressing wave contribution to the detuning.

B. Viscous rescaling

It is convenient to introduce a viscous scaling for Eqs. (75)–(77a),

$$\bar{\chi} = (2/\sqrt{S})(\epsilon_c/\epsilon)\chi = (2/\sqrt{S})\epsilon_c x , \tag{78a}$$

$$\bar{T} = (\epsilon_c/\epsilon)^2 T = \epsilon_c^2 t , \tag{78b}$$

$$\bar{A} = (\epsilon/\epsilon_c)(|J_b|/2)^{1/2} A , \tag{78c}$$

where ϵ_c, the internal viscous scale, is given by

$$\epsilon_c = \left\{ \frac{2}{\mathrm{Re}} + \frac{1}{(2\,\mathrm{Re})^{1/2}} \cdot \left[\frac{1}{\sinh(2d)} + \frac{1}{N\pi}\left(1 - \frac{2d}{\sinh(2d)}\right)\right]\right\}^{1/2}. \quad (79)$$

This yields the rescaled NLS equation

$$i\bar{A}_{\bar{T}} = \bar{A}_{\bar{\chi}\bar{\chi}} + (\Lambda - i)\,\bar{A} \pm \bar{A}\,|\bar{A}\,|^2, \quad (80a)$$

with boundary conditions

$$\bar{A}_{\bar{\chi}} = -\hat{R}\bar{A}^* - \hat{D}\bar{A}, \quad \text{at } \bar{\chi} = 0, \quad (80b)$$

$$\bar{A} \to 0, \quad \text{as } \bar{\chi} \to \infty. \quad (80c)$$

The sign of the nonlinearity in (80a) is chosen to be the same as the sign of J_b. There are now three parameters in Eqs. (80): a ratio of scaled forcing amplitude to the internal viscous scale,

$$\hat{R} = (\sqrt{S}/2)(\epsilon/\epsilon_c)R, \quad (81a)$$

the ratio of wavemaker viscous damping and detuning (which is a result solely of the meniscus layer at the wavemaker) to the internal viscous scale,

$$\hat{D} = \frac{1-i}{\epsilon_c(2S\,\mathrm{Re})^{1/2}}, \quad (81b)$$

and a detuning scaled by the viscous damping,

$$\Lambda = \epsilon_c^{-2}\left[(\sigma - \sigma_0)/\sigma_0 + \Lambda_v + (\epsilon^2/2)J_a e^{2\gamma_R X}\right]. \quad (82)$$

There are three contributions to the detuning (82). The first comes from variations in the forcing frequency. The second,

$$\Lambda_v = \mathrm{Im}\{\epsilon^2 D_0\} = \frac{1}{(2\,\mathrm{Re})^{1/2}}\left[\frac{1}{\sinh(2d)} + \frac{1}{N\pi}\left(1 - \frac{2d}{\sinh(2d)}\right)\right], \quad (83)$$

is induced by the viscous effects. The third term in (82) is the result of the interaction with the slowly decaying progressing wave; in practice, this term is small and will be neglected in the linear analysis performed below.

By considering the size of their contributions to ϵ_c, the relative importance of the viscous boundary layers at the side walls, bottom, and free surface can be determined; this is a useful method of comparing experimental facilities. When $d \gg \frac{1}{4}\ln(8\,\mathrm{Re})$, the damping resulting from the bottom can be neglected, relative to that of the surface; in this case, the channel will be considered deep. Similarly, when $N \gg \sqrt{2\,\mathrm{Re}}(2-S)/\pi$, the side wall damping (including the meniscus layer) can be neglected and the channel can be considered wide. In a deep, wide tank, the damping from the free surface will dominate at $\epsilon_c \sim \sqrt{2/\mathrm{Re}}$. The magnitude of ϵ_c scales the critical value of forcing at which cross-waves appear (through $\hat{R}$), the width over which resonance is observed (through Λ), and the skewedness of the neutral stability curve (through $\hat{D}$).

C. Linear analysis

For a small cross-wave amplitude, such that the nonlinear term can be neglected, the problem (80) is reduced to a linear theory that is amenable to analysis.[2,12] The most unstable eigenmode is given by

$$\bar{A} = \bar{A}_0 e^{h\bar{\chi} + q\bar{T}}, \quad (84)$$

where

$$h = h_r + ih_i = [i(1+q) - \Lambda]^{1/2}, \quad h_r < 0, \quad (85)$$

and $\bar{A}_0$ is a complex constant. The growth rate q is specified by the implicit equation

$$\hat{R}^2 = [\Lambda^2 + (1+q)^2]^{1/2} + |\hat{D}|\,[\sqrt{2}(h_r + h_i) + |\hat{D}|]. \quad (86)$$

By setting $q = 0$ in Eq. (86), an expression for the neutral stability curve for the linear excitation of cross-waves is obtained. In Fig. 1, neutral stability curves are drawn in the $(\Lambda, \hat{R}^2)$ plane for various values of the $|\hat{D}|$. Note that in the limit of a wide, deep tank, $|\hat{D}|$ approaches its maximum value of $1/\sqrt{2}$; this corresponds to a curve of maximum skewedness. For tanks that are not both deep and wide, $|\hat{D}| \sim 1/\sqrt{\mathrm{Re}} \ll 1$, and the wavemaker viscous effects can be ignored. In this case, the stability curve is symmetric.[12]

Note also that the neutral stability curves all lie above $\hat{R} = 1$; this can be interpreted as the existence of a viscous threshold for linear instability to cross-waves, i.e., the scaled forcing amplitude, $\epsilon R\sqrt{S}/2$ must be greater than the internal viscous scale ϵ_c for transition to occur.

D. Nonviscous dissipation

In this paper the effects of nonzero viscosity have been incorporated into the cross-wave analysis. A further refinement, necessary to describe the evolution in many geometries, would be to include the effects of surface contamination and surface tension, including capillary hysteresis.[10,18] As the vorticity would still be contained within small boundary layers, it is our belief that these effects can be treated within the framework of the matched asymptotic methodology applied here.

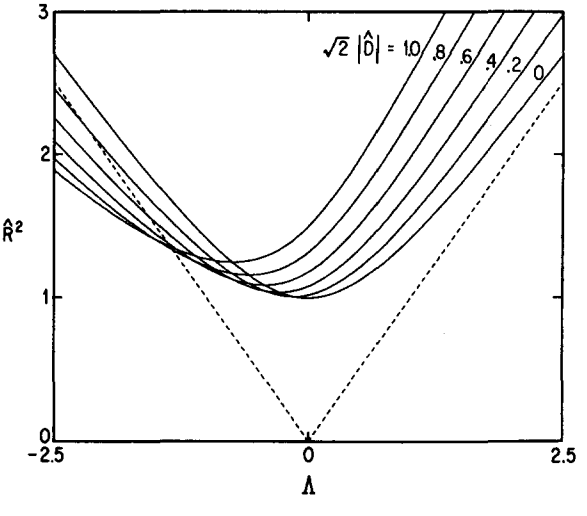

FIG. 1. The neutral stability of cross-waves as a function of detuning Λ and scaled forcing squared $\hat{R}^2$ for various values of the damping ratio $|\hat{D}|$. Instability occurs above these curves. The dashed lines (- - -) represent the inviscid theory. In the case of a tank, not both deep and wide, $|\hat{D}| = 0$ and the neutral stability curve is symmetric; instability first occurs at zero detuning and $\hat{R}^2 = 1$. As the damping ratio increases, wavemaker damping becomes more important, the neutral stability curve becomes more skewed, and onset occurs for larger forcing amplitudes. Note that for $|\hat{D}| \neq 0$, the minimum is shifted from the inviscid cutoff frequency.

The addition of surface contamination leads to a modification of the free-surface boundary layer structure. Models of miscible and immiscible surface contaminants that spread uniformly may promote the order of the free-surface contribution from $1/\mathrm{Re}$ to $1/\sqrt{\mathrm{Re}}$.[10]

Incorporation of surface tension effects is particularly important for geometries in which the characteristic length scales are less than a few centimeters. Surface tension modifies the dispersion relationship and consequently changes the coefficients in the governing nonlinear Schrödinger equation.[6] A more formidable problem is the addition of capillary hysteresis; a preliminary model of this phenomenon has been proposed by Hocking.[18] Because of the singular behavior of the contact angle, this phenomenon's modification of the evolution equations is difficult to predict.

VII. CONCLUSIONS

In summary, the results here allow a precise determination of viscous damping in wave tanks of arbitrary dimension: the relative viscous contributions from the free-surface, side wall, bottom, and wavemaker can be computed. It is necessary to modify the Havelock[14] solution to include a slow decay of the progressing wave. The modification of the wavemaker boundary conditions leads to a skewing of the neutral stability curves; this effect, which is observed experimentally, will be examined in more detail in future work. This work also allows the quantitative determination of the viscous contributions to the heuristic linear damping and detuning suggested by previous authors. By incorporating and expanding the ideas of Mei and Liu,[9] a methodology for the modulation theory for viscous cross-waves has been presented. By using the Green's identity for the solvability condition, Jones' method[2] is shortened considerably. This methodology can be applied to viscous effects in related problems. In addition, the formalism developed here will hopefully allow the inclusion of nonviscous effects, which are important in many geometries.

ACKNOWLEDGMENTS

The authors thank Connie Spencer for her critical evaluation of an early version of this manuscript.

This work was supported by the National Science Foundation Grant No. MSM-8611379, the Office of Naval Research Contract No. N00014-86-K-0617, and AFOSR Contract No. F49620-86-C0130.

APPENDIX A: THE HAVELOCK SOLUTION

The solution to the wavemaker problem specified by (34) and (35), in the inviscid limit, was considered by Havelock.[14] The solution can be found as a sum of eigenmodes of the Laplacian satisfying the free-surface and bottom boundary conditions,

$$\phi_i = Be^{-imx}\frac{\cosh m(z+d)}{\cosh md} + \sum_j iB_j e^{-m_j x}\frac{\cos m_j(z+d)}{\cos m_j d}, \tag{A1}$$

where m and m_j must satisfy the eigenvalue relationships

$$mH\tanh(md) = 4, \quad m>0, \tag{A2a}$$

$$m_j H\tan(m_j d) = -4, \quad m_j>0, \tag{A2b}$$

and B and B_j are unknown coefficients to be determined. The first term in (A1) represents a progressing wave traveling away from the wavemaker; the corresponding solution, representing a wave moving toward the wavemaker, can be neglected by imposing a radiation condition or, equivalently, adding a small amount of dissipation and requiring that the disturbance decay for large x. The remaining terms in (A1) represent "parasitic modes," localized eigenmodes that decay exponentially with distance from the wavemaker.

The coefficients B and B_j are determined by the inhomogeneous wavemaker boundary condition (35b); the inhomogeneity must be projected onto the eigenmodes at $x=0$. This yields[14]

$$B = 8H/[(16d-4H)m - m^3H^2d], \tag{A3a}$$

$$B_j = 8H/[(16d-4H)m_j + m_j^3H^2d]. \tag{A3b}$$

It is desirable to incorporate leading-order viscous effects into the solution ϕ_i. The viscous damping of the parasitic modes introduces an order $(\epsilon\delta)$ local correction and can safely be neglected. However, the progressing wave's amplitude will decay and be detuned on a length scale that may be comparable to that of the cross-wave. To incorporate this fact, the amplitude, B, is multiplied by a complex exponential acting on the long length scale χ, i.e., $B\to Be^{\gamma x}$. The constant γ can easily be computed from (34) and (35a)–(35e), and is given in (37). The interested reader is directed to the work of Mei and Liu[9] for details.

1. Computation of R

In Sec. IV D the computation of R, the effective forcing, is reduced to evaluating certain integrals of ϕ_i. These are evaluated below. First, note that

$$\phi_{i_{xx}} = -\phi_{i_{zz}}, \tag{A4}$$

therefore

$$\int_0^L \phi_{i_{zz}}\,dx = -\int_0^L \phi_{i_{xx}}\,dx = \phi_{i_x}\int_0^L = i + O(\epsilon\delta), \quad \text{at } z=0, \tag{A5}$$

where the slow decay of the progressing wave has been used to eliminate the contribution from the far end $(x=L)$ and the small error is introduced by the viscous effects.

The evaluation of the second integral is much more difficult. To this end, we introduce, *deus ex machina*, a contour integral for ϕ_i,

$$\phi_i = \int_\Gamma e^{-qx}\Phi(q,z)\,dq, \tag{A6}$$

where

$$\Phi(q,z) = -\frac{1}{\pi q^2}\left(\frac{\cos q(z+d)}{\cos qd}\right)\frac{4}{Hq\tan qd + 4} \tag{A7}$$

and Γ is the contour that starts at $-i\infty$, follows the imaginary axis to $+i\infty$, and is indented into the right half-plane

at $-im$ and 0 and into the left half-plane at $+im$. The reader is invited to demonstrate that expressions (A1) and (A6) are equivalent by closing the contour Γ through the right half-plane and summing over the residue for the poles at $q = im, m_j$.

To evalute the integral in (58), note that

$$\lim_{L\to\infty}\int_0^L \phi_i\, dx\Big|_{z=0} = \int_\Gamma \frac{1}{q}\Phi(q,0)dq\,. \tag{A8}$$

Because $\Phi(-q,0) = \Phi(q,0)$, the integral on Γ vanishes as a result of symmetry everywhere, except on the indentation at the origin. Consequently, the contour Γ can be replaced by a semicircle around the origin, or, using symmetry again, half the value of a loop around the origin,

$$\begin{aligned}\lim_{L\to\infty}\int_0^L \phi_i\, dx\Big|_{z=0} &= \frac{1}{2}\oint_{q=0} dq\,\frac{1}{q}\Phi(q,0)\\ &= -\oint\frac{dq}{2\pi q^3}\left(\frac{4}{4+Hq^2d+O(q^4)}\right)\\ &= -\oint\frac{dq}{2\pi q^3}\left(1-\frac{H\,dq^2}{4}+O(q^4)\right) = \frac{iHd}{4}\,,\end{aligned} \tag{A9}$$

where the last step is evaluated using Cauchy's residue theorem. This identity allows R to be expressed in closed form in Sec. IV D.

APPENDIX B: SECOND-ORDER SOLUTION

In this appendix the portion of ϕ_2 that contributes to resonances in the interior of the fluid are computed. As discussed in the text, nonresonant terms, terms that are localized on the wavemaker and consequently contribute only to the boundary condition, and higher-order viscous corrections, are not reported here; most of these terms have been computed[16] and are small compared to those retained. Following (50), a solution of the form

$$\begin{aligned}\phi_2 = {}&\phi_{21}e^{it} + \phi_{22}e^{2it} + \phi_{23}e^{3it}\\ &+ \phi_{24} + \text{c.c.} + \text{nondominant terms}\end{aligned} \tag{B1}$$

is solved for below.

1. ϕ_{21}: Resonant interaction

The resonant contribution at second order ϕ_{21} was considered in Sec. IV. Because the first-order solution ϕ_1 contains no terms constant in time, ϕ_{21} cannot contribute to resonance at third order and, as such, it is not computed here.

2. ϕ_{22}: Cross-wave–cross-wave interaction

Naively, one might guess that cross-wave–cross-wave interactions lead to components with constant and $e^{\pm 2it}$ time dependence; however, the constant term vanishes.[2] The remaining component ϕ_{22} satisfies the homogeneous problem (38) and (39b)–(39e), together with the free-surface boundary condition

$$\begin{aligned}H\phi_{22_z} - 4\phi_{22} = {}&-(i/2)[1+3H^{-2}\\ &+3(H^{-2}-1)\cos(2y)]A^2\,, \quad \text{at } z=0.\end{aligned} \tag{B2}$$

This can be solved for directly.[2,16] The solution is given by

$$\begin{aligned}\phi_{22} = {}&(i/8)[1+3H^{-2}+3H^2(H^{-4}-1)\\ &\cdot\cos 2y\,\{\cosh[2(z+d)]/\cosh(2d)\}]A^2\,.\end{aligned} \tag{B3}$$

3. ϕ_{23}: Cross-wave–progressing wave interaction

The cross-wave–progressing wave interaction has two pieces: a resonant portion ($e^{\pm it}$), considered in ϕ_{21}, and a nonresonant portion ϕ_{23}, with time dependence like $e^{\pm 3it}$, considered here. We see that ϕ_{23} satisfies the homogeneous problem (38) and (39b)–(39e), together with the free-surface boundary condition

$$\begin{aligned}H\phi_{23_z} - 9\phi_{23} = {}&iAe^{\gamma x}e^{-imx}\\ &\times\cos y(2+m^2-42H^{-2})\,, \quad \text{at } z=0\,.\end{aligned} \tag{B4}$$

A solution can be found in the same fashion as the Havelock solution in Appendix A.[2,16]

$$\begin{aligned}\phi_{23} = {}&iAe^{\gamma x}e^{-imx}\cos y\\ &\cdot[\cosh s(z+d)/\cosh sd\,]\\ &\cdot\{2+m^2-42H^{-2}/[sH\tanh(sd)-9]\}+\tilde{\phi}_{23}\,,\end{aligned} \tag{B5}$$

where

$$s = \sqrt{m^2+1}\,. \tag{B6}$$

The correction $\tilde{\phi}_{23}$ is localized near the wavemaker and corresponds to the parasitic modes in the Havelock solution. It will only yield a higher-order correction to the wavemaker boundary condition, and, as such, need not be computed.

4. ϕ_{24}: Progressing wave–progressing wave interaction

The progressing wave–progressing wave interaction contains two components. A term with time dependence like $e^{\pm 4it}$ occurs; because the first-order solution only has terms like $e^{\pm it}$ and $e^{\pm 2it}$, no resonance can occur. The second component has terms that are constant in time; however, these terms all cancel.[2,16] This leads to the conclusion

$$\phi_{24} = 0\,. \tag{B7}$$

The expressions for ϕ_2 can now be used to compute the solvability condition on ϕ at third order.

[1] C. J. R. Garrett, J. Fluid Mech. **41**, 837 (1970).
[2] A. F. Jones, J. Fluid. Mech. **138**, 53 (1984).
[3] B. J. S. Barnard and W. G. Pritchard, J. Fluid Mech. **55**, 245 (1972).
[4] B. J. S. Barnard, J. J. Mahony, and W. G. Pritchard, Philos. Trans. R. Soc. London Ser. A **286**, 87 (1977).
[5] S. Lichter and J. Chen, J. Fluid Mech. **183**, 451 (1987).
[6] J. Miles and J. Becker, J. Fluid Mech. **186**, 129 (1988).
[7] F. Ursell, Proc. R. Soc. London Ser. A **214**, 79 (1952).
[8] H. Lamb, *Hydrodynamics* (Cambridge U.P., Cambridge, 1932), 6th ed.
[9] C. C. Mei and L. F. Liu, J. Fluid Mech. **59**, 239 (1973).
[10] J. W. Miles, Proc. R. Soc. London Ser. A **297**, 459 (1967).

[11]L. Shemer and S. Lichter, Phys. Fluids **30**, 3427 (1987).
[12]S. Lichter and A. J. Bernoff, Phys. Rev. A **37**, 1663 (1988).
[13]J. Chen, S. Lichter, and A. J. Bernoff, submitted to Phys. Fluids A.
[14]T. H. Havelock, Philos. Mag. **8**, 569 (1929).
[15]C. C. Mei, *The Applied Dynamics of Oean Surface Waves* (Wiley, New York, 1982).
[16]L. P. Kwok, Ph.D. thesis, University of Arizona, 1988.
[17]A. Larraza and S. Putterman, J. Fluid Mech. **148**, 443 (1984).
[18]L. M. Hocking, J. Fluid Mech. **179**, 253 (1987).